Jinst
PUBLISHED BY IOP PUBLISHING FOR SISSA MEDIALAB
RECEIVED: *November 8, 2019*
ACCEPTED: *December 11, 2019*
PUBLISHED: *January 22, 2020*

2020 JINST 15 P01026

Development and validation of a CFD-enabled digital twin of a portable HPGe gamma spectrometer

M. Jeltsov,[a] P. Priimagi,[a] V. Malgin,[b] O. Yakovlev[b] and A.H. Tkaczyk[a,c,1]

[a] *Estflow Consulting OÜ,*
Narva maantee 9, EE-51013, Tartu, Estonia

[b] *Baltic Scientific Instruments (BSI),*
Ramulu street 3, LV-1005, Riga, Latvia

[c] *Institute of Technology, University of Tartu,*
Nooruse 1, EE-50411, Tartu, Estonia

E-mail: alan@ut.ee

ABSTRACT: This paper presents the design of an easily portable spectrometer using high purity germanium (HPGe) detector — HandSpec. The key challenge in the design of a lightweight spectrometer is to minimize its heat losses so that efficient electric cooling could be used instead of bulky dewars. The design process has been largely based on experimental investigations. In this study, a *digital twin* of the HandSpec cryostat using computational fluid dynamics (CFD) method is developed to support the design and optimization of the physical prototype.

KEYWORDS: Cryogenics and thermal models; Detector design and construction technologies and materials; Gamma detectors (scintillators, CZT, HPGe, HgI etc); Simulation methods and programs

[1] Corresponding author.

https://doi.org/10.1088/1748-0221/15/01/P01026

Contents

Abbreviations:
HPGe — High Purity Germanium
HADEDE — HAnd-held DEtector Design
SME — Small and Medium Enterprise
BSI — Baltic Scientific Instruments
CFD — Computational Fluid Dynamics
CAD — Computer-Aided Design

1 Introduction

High Purity Germanium (HPGe) detectors are used in spectrometers due to their high energy resolution, efficiency and sensitivity to ionizing radiation, particularly X-rays and gamma rays [1, 2]. However, to reduce the electrical noise to an acceptable level for high-quality spectroscopic data, germanium detectors must be cooled down to cryogenic temperatures (typically below 120 K) [3].

The simplest and most common way to cool the detector is to use cryostats with liquid nitrogen (77°K) called *dewars*. However, since the dewar systems are rather bulky and heavy they are not easily transportable in the field. Therefore, portable devices are required to improve the operational flexibility and functionality of radiation monitoring systems. Recent advancements in mechanical cooling technologies have made it possible to design battery powered, truly man-portable systems using Stirling cryocoolers [1, 4–7]. One of the main objectives for practical applications is to design

2020 JINST 15 P01026

spectrometers with short cool-down time from room temperature to cryogenic temperatures [8]. This means that the heat transfer from ambient has to be minimized.

The design of compact portable spectrometers has to satisfy several criteria including manufacturability, assembly, functionality, data quality, operational duration, user-friendliness which makes the development process inherently iterative. With advancements in computers and numerical models, computational fluid dynamics (CFD) has become a useful tool in the design and optimization of physical products and processes. Numerical modeling or CFD allows evaluating a large number of prototype configurations at a wide range of operating conditions at much faster pace. Moreover, numerical models with detailed resolution can provide much more information than physical measurements. In a design and optimization study of a composite HPGe detector, Kojouharov et al. [9] studied the temperature distribution and warm up/cool down transients using numerical simulations with ANSYS. A potentially important effect of residual gases in vacuum, however, was not addressed in their work.

In the HADEDE project, two Baltic SMEs, Estflow and BSI, have designed and optimized a maintenance-free man-portable (lightweight), long-lasting spectrometer called HandSpec. The design uses electromechanical cryocooler based on low-power Stirling engine. In cooperation, a prototype is developed with minimum heat losses that would allow for minimum cooling power and maximum operating time. The low cooling power (typically 1–3 W@80K) limits the permissible heat losses in the chamber defined by the design of cryostat and level of vacuum within.

In the HandSpec spectrometer, an HPGe detector is placed into an aluminum container and fixed to the cryostat body by support rings, providing structural support and separating thermally the detector unit from the warm outer walls. The container is placed under vacuum to minimize heat losses. Cooling power is generated in the cold finger with cold tip as the coldest part. Figure 1 shows the actual spectrometer prototype along with its CAD drawing.

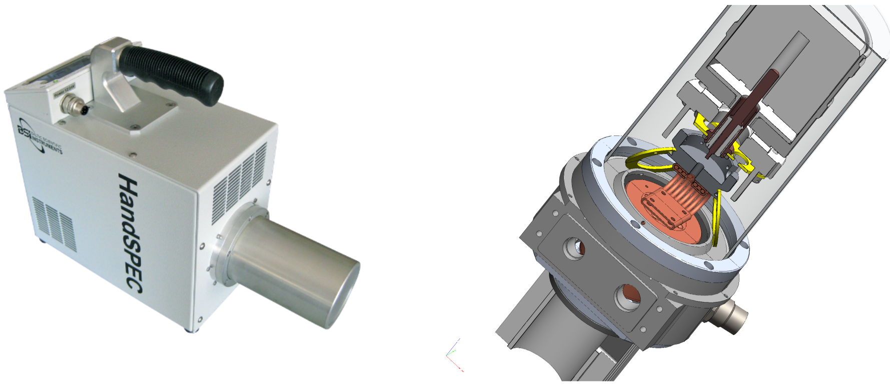

Figure 1. HandSpec prototype (left) and a cross-section of the CAD model of it (right).

For a good thermal insulation design for an energy-efficient spectrometer, simulation and analysis of the heat losses in the vacuum chamber of portable devices are the most important criteria.

After this introduction, a brief overview of different heat transfer mechanisms is provided in section 2. CFD model of the HandSpec spectrometer is described in section 3. The results of CFD simulations and comparison with experimental measurements where possible is provided in section 4. Finally, in section 5 some conclusions of the development process are given and the potential future activities are discussed.

2 Heat transfer mechanisms in HandSpec

The total heat transfer from the ambient environment through the spectrometer to the cooler, Q_{tot}, takes place via three distinct mechanisms: conduction in solids Q_{cond}, conduction in residual gases Q_{resid} and thermal radiation Q_{rad} [3, 10]:

$$Q_{\text{tot}} = Q_{\text{cond}} + Q_{\text{resid}} + Q_{\text{rad}} \tag{2.1}$$

In order to provide practical suggestions to improve the spectrometer thermal performance, it is important to know the relative importance of each phenomenon.

Conduction through solid structures (i.e. cryostat body, support structures, instrumentation wiring, beam pipes) is described by the Fourier Law:

$$q_{\text{cond}} = \lambda * \nabla \text{T} \tag{2.2}$$

where q_{cond} is heat flux (W/m^2), λ is the thermal conductivity of the material (W/m/K) and ∇T is the temperature gradient. It must be noted that λ varies with temperature and since the temperature variations in HPGe spectrometers are large this dependency is taken into account in modeling.

Conduction in the rarefied gas environment occurs due to residual gases present in the imperfect vacuum, leakage through seals and/or outgassing from the internal surfaces. The amount of heat transferred by this mechanism depends on the concentration of residual gases (corresponds to the vacuum pressure level) and temperatures of the container walls. The operating pressure in the cryostat with HPGe detector is usually in range 1E-5–1E-3 mbar. Higher pressures may lead to excessive convective heat transfer as well as contamination of the HPGe detector.

Thermal radiation plays an important role in systems with high-temperature difference. This can be reduced by using surface treatments such as polishing, multilayer insulation and thermal shielding.

Radiation heat flux, emitted from and absorbed by a surface, q_{rad} can be modelled using the Stefan-Boltzmann law:

$$q_{\text{rad}} = \sigma T^4 \tag{2.3}$$

where σ is the Stefan-Bolzmann constant.

In real applications however, heat flux incident on a surface can be absorbed, reflected or transmitted. These effects are taken into account using empirically determined absorptivity (α), reflectivity (ρ) and transmissivity (τ) coefficients on spectrometer surfaces. These coefficients depend on surface roughness, temperature, incident angle, radiation wavelength. Therefore, it is important to evaluate their sensitivity on the spectrometer performance.

3 Numerical analysis of heat transfer in HandSpec

A three-dimensional CFD model of the spectrometer was created to carry out detailed steady-state and transient analysis of the heat transfer within the device, more specifically, the conductive and radiative heat transfer from the ambient environment to the cryocooler.

2020 JINST 15 P01026

The motivation behind this study is to better understand the thermal behavior of the HandSpec spectrometer in terms of three-dimensional temperature profiles, the individual contribution of the different heat transfer mechanism, their dependence on the system configuration parameters and their effect on the device performance i.e. required cooling power. The objective is to build a detailed CFD model that would take into account the relevant physical processes as accurately and as practically as possible and simulate the steady state and transient heat transfer processes to provide means for optimization of the device to minimize the required cooling power.

Pre-processing of geometry, meshing, physics modeling, simulation and post-processing of the results are all done with Star-CCM+ (version 13.02).

The model is gradually developed in terms of fidelity of the geometry and physics representations (different energy transfer models):

- Stage 1 — Conduction through spectrometer structures only; quick verification of the modeling parameters, i.e. mesh study, is also performed.
- Stage 2 — Conduction + Radiation (between the inner surfaces of the container).
- Stage 3 — Conduction + Radiation + Residual Gas Convection (in the volume inside the spectrometer container).

This step-wise approach for increasing model complexity (inclusion of heat transfer mechanisms) allows us to address individual heat transfer mechanisms separately, evaluate their relative effect, verify model setup and thereby increase confidence in the numerical modeling.

3.1 Geometry and mesh

An external and cross-section view of the full spectrometer CAD model is shown in figure 2. The CFD model includes all components of the spectrometer except electric leads, cryocooler, gas getters, detector internals and nuts/bolts.

For a numerical solution, the domain is divided into a finite number of small volumes or mesh. In order to quantify and minimize errors from such spatial discretization, a mesh sensitivity study is carried out. Three meshes with different resolutions are shown in figure 3 (top images). Meshes were designed so that the mesh with the largest element size would still represent the geometric details in the model.

In order to quantify and minimize the effect of numerical discretization on the results a solution verification exercise (mesh study) was carried out. In this study, only conduction in solid structures was considered. The resulting temperature fields and cooling powers are very similar in all the cases with small variations in certain aspects i.e. heat losses through the support rings (see bottom images in figure 3). The heat transfer due to conduction is around 0.1 W which is in accordance with analytic estimates provided earlier. Note that conduction is a small contributor to the total heat losses which are expected to be around 2 W (estimate from earlier physical tests as well as a requirement for a transportable device). The mesh with 3 cm base size was selected considering the fidelity of geometrical representation and computational efficiency.

2020 JINST 15 P01026

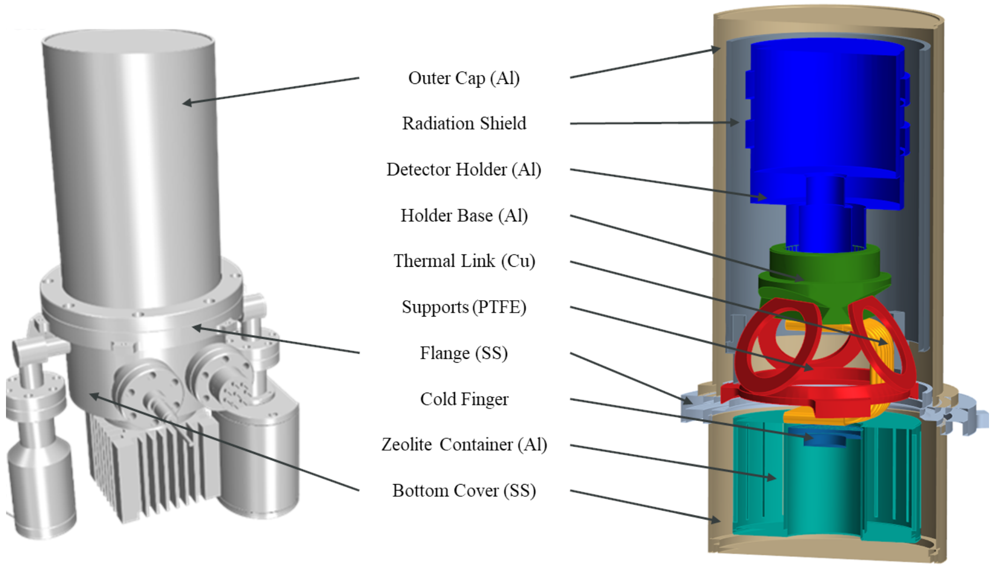

Figure 2. An external and cross-section views of the cryostat CAD model in the CFD software.

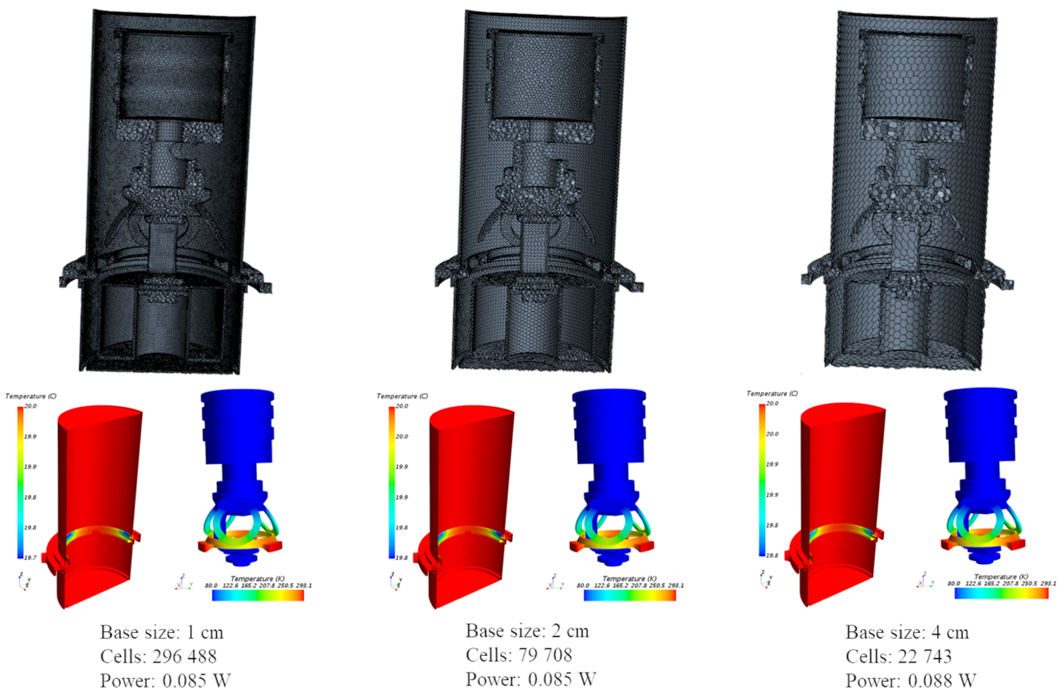

Figure 3. Mesh sensitivity study.

Moreover, to model the residual gas conduction effects in the cryostat, the vacuum domain was extracted as the internal volume of the spectrometer using the solid structures as boundaries. The interfaces between the vacuum domain and the solid structures were defined for conjugate heat transfer analysis.

3.2 Physics models and solvers

Conduction. Conduction heat transfer through solids (and in the rarefied gas environment) is modeled using segregated energy model. This model calculates the temperature distributions in different parts with different materials in the spectrometer — aluminum, stainless steel, copper, PTFE.

Radiation. Thermal radiation in the system is modeled using the Surface-to-Surface (S2S) radiation model which relies on an advanced numerical scheme to analyze the radiative heat transfer between the surfaces of arbitrary complexity that form enclosed space inside the spectrometer [11].

The radiation properties and the thermal boundary conditions that are imposed on each surface define uniquely the amount of radiation that a surface receives and emits. The surface properties are quantified in terms of emissivity, reflectivity, transmissivity, and radiation temperature.

During the radiation model development for cryostat modelling the initial parameters for different materials were defined.

Residual gas conductivity. Heat transfer due to residual gases in the vacuum domain is calculated according to the temperatures on the surrounding walls and the heat transfer coefficient inside the gas space. The domain is defined as a non-flowing material domain activating only energy equation i.e. convection is excluded (note that at operating conditions the pressure inside the cryostat is below 1E-2 mbar). The density of the rarefied gas is calculated by the Ideal Gas Law. A thermal conductivity coefficient is used to model the effective heat transfer within the vacuum domain. However, as the model does not calculate the gas conductivity a relationship between the residual gas conductivity, temperature and pressure is empirically defined. The values of thermal conductivity used in this study ranged from 0.0001 to 0.01 W/m/K.

A fluid-solid temperature jump condition has been defined at the inner surface of the cryostat (similar to the Maxwell slip for friction) according to the theory developed by Von Smoluchowski and implemented in Star-CCM+ [4, 5].

Material properties. The model consists of a variety of different materials whose physical properties need to be defined carefully to have realistic simulation results. Selected values for different materials used in the cryostat model together with the other physical properties can be found in table 1.

Table 1. Physical properties of materials.

Material	Density (kg/m^3)	Thermal conductivity (W/m/K)	Specific heat capacity (J/kg/K)
PTFE	2160	0.3	1200
Al, $AlMg_3$	2702	237	905
Cu	8940	398	386
SS316	8000	15	480
Residual gas	Ideal Gas Law	0.001	0

2020 JINST 15 P01026

The initial temperature of all detector parts was set to 293 K corresponding to the ambient temperature used in all simulations. Materials properties contribute to the list of uncertain model parameters that have been calibrated using experimental observations from the prototype.

3.3 Boundary conditions

Boundary conditions were defined so that the results depend only on the heat transfer phenomena within the spectrometer itself and not on the conditions at the ambient environment (i.e. external heat transfer coefficient).

Therefore, the temperature of the external walls is set to a defined ambient temperature of 20°C (actual distribution is anyway expected to be somewhat uniform). The temperature at the tip of the cold finger connected to the cooler (i.e. the coolest surface in the model) is set to the desired value of 80 K. For this particular case, depending on the geometry and physics used in the model the total heat transfer through the system is calculated.

Moreover, it is possible to simply monitor the heat transfer rate through different interfaces to evaluate integral and local heat balance for convergence as well as identify the required cooling power.

In order to understand the performance of the numerical (and physical) model, it is important to define the parameters that need to be monitored during calculations. For our purposes, these include temperature values and heat fluxes in certain locations inside the device, for example detector temperature (K), total energy loss (W), support ring heat loss (W), radiative heat transfer on the detector container (W), and radiation emission from top cover (W).

Radiation properties are set on all surfaces. On the external walls, the emissivity is set to 0 and reflectivity to 1 i.e. radiation heat transfer with the environment is discarded. All emissivity values used for the internal parts can be seen in figure 4.

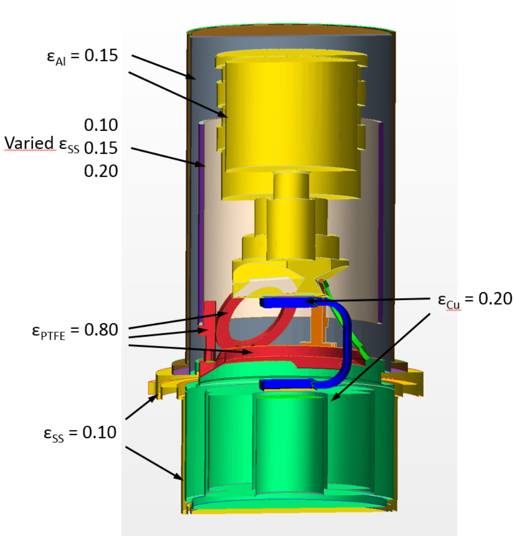

Figure 4. Emissivity values of different surfaces used ($\varepsilon_{\mathrm{Al}}$ — aluminum surfaces, $\varepsilon_{\mathrm{SS}}$ — stainless steel surfaces, $\varepsilon_{\mathrm{PTFE}}$ — PTFE surfaces, $\varepsilon_{\mathrm{Cu}}$ — copper surfaces).

4 Results

4.1 Contribution of different heat transfer mechanisms

As shown in figure 5, the hottest part of the spectrometer is its external container. The coldest part, tip of a cryocooler, is located inside the spectrometer connected to the detector unit by a copper braid. Internal components supporting the detector unit in its position and the vacuum environment accommodate the thermal gradient.

The detailed 3D CFD model provides important insights into the radiation heat transfer phenomenon. It was observed that while the outer components of the spectrometer constitute the major heat emission (top cover, bottom cover, are practically at ambient temperature of 300 K) the smaller inner parts of the detector (holder insulator, support rings) absorb and emit heat depending on the spatial temperature distribution and the view factors with respect to other components. This effect is explained by the fact that the temperature of the "middle" parts (detector holder and support ring) is on average lower than the outer parts (300 K) and higher than the "inner" parts closest to the cooler (such as detector which is at about 80 K).

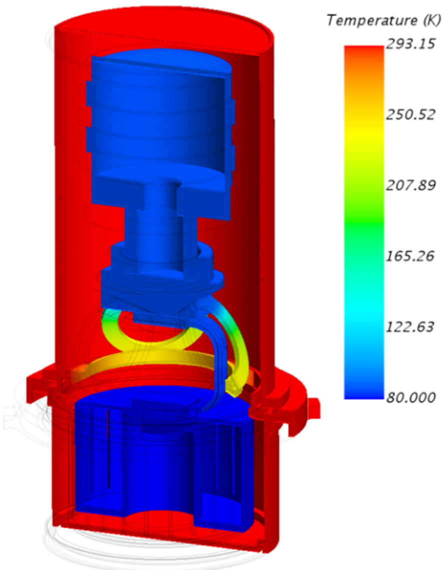

Figure 5. A representative temperature distribution in HandSpec spectrometer.

In a converged solution the heat entering through outer surfaces must equal to the heat exiting through the cooler (shown in overlapping blue and green lines). This total heat transfer rate is calculated to be approximately 2.6 W. Conduction is measured at the contacts (includes three locations) between the flange and holder insulator and equals to about 0.25 W. Note that this value is affected by the thermal conduction in the residual gases through the overall temperature profile — the higher the conduction in the gas the higher the conduction in this solid contact. Radiation shows the total radiation heat flux coming from the inner surfaces of the outer parts and is about 1.5 W. The difference between the total heat transfer and the conduction + radiation represents the residual gas conduction heat transfer, about 0.85 W in the base model.

2020 JINST 15 P01026

4.2 Effect of radiation shield, its height and residual gas conductivity

In order to minimize direct heating of the detector by the radiation, a special shield is proposed to be installed in the space between the spectrometer housing and the detector. In addition to the uncertainty in the surface emissivity, the shape and size of the shield could also be optimized for best performance.

In order to quantify the effect of radiation shield and its height as well as to identify whether there is an optimum configuration, models without shield, 50% and 75% of the nominal height and full height were built (see figure 6). The emissivity of the shield and detector container were 0.1 and 0.15, respectively.

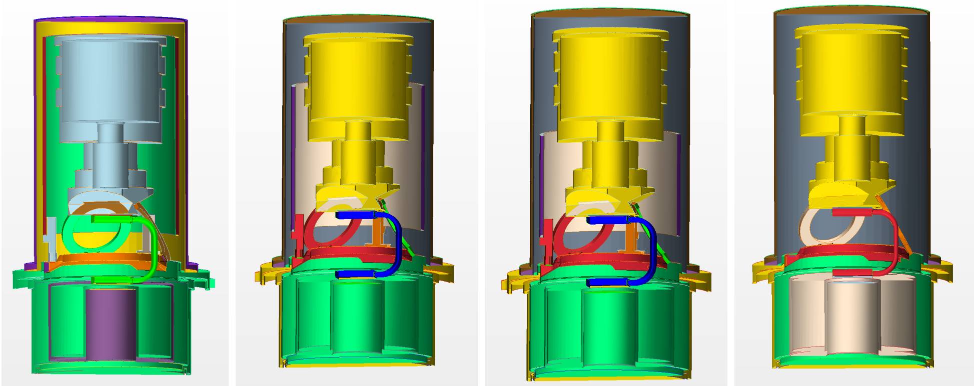

Figure 6. Cryostat models with full shield, 3/4, 1/2 of the shield height and model without a shield.

The analysis was made for three different vacuum conductivity levels (0, 0.001 and 0.005 W/m/K). Required cooling power was calculated for every shield configuration. Figure 7 shows that the required cooling power increases monotonically with both shield height as well as with the residual gas conductivity i.e. vacuum quality. Moreover, the level of vacuum is regarded as more important considering the efficiency of the spectrometer.

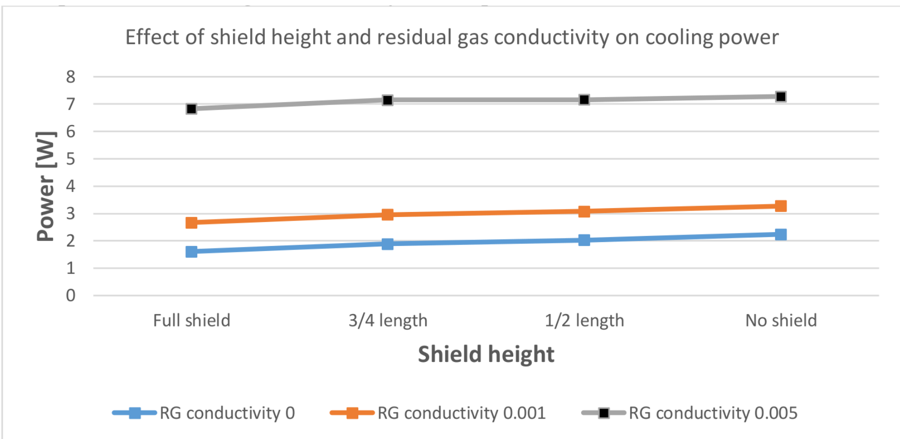

Figure 7. Effect of shield height and residual gas conductivity on the total cooling power.

2020 JINST 15 P01026

Quantitatively, the relative effect between the full-length shield and no shield situation increases with vacuum level. Full-length shield reduces the cooling power about 28% at ideal when the residual gas conductivity is zero (ideal vacuum) whereas with the highest RG conductivity (lowest vacuum level) only 16% is gained when compared to the no-shield situation. This brings us to two conclusions:

- In order to lower cooling power, a good vacuum is very important, and
- At a high level of vacuum, the shield provides further significant gain in its efficiency.

Same tendencies were found in the systems with the higher (0.15 and 0.20) shield emissivity values.

4.3 Effect of shield surface emissivity

During modeling, it was observed that the overall heat transfer is affected by surface radiation parameters, namely emissivity. Therefore, cases with shield surface emissivity of 0.1, 0.15 and 0.2 (less than, equal to and larger than the aluminum detector housing surface emissivity) are simulated and compared. All other parameters were unchanged with the emissivity values $\varepsilon_{\text{aluminum}} = 0.15$, $\varepsilon_{\text{SS}} = 0.10$, $\varepsilon_{\text{Cu}} = 0.20$ and $\varepsilon_{\text{PTFE}} = 0.80$. The results shown in figure 8 indicate that the emissivity value of the shield is not too influential on the total cooling power (at least not within the studied range).

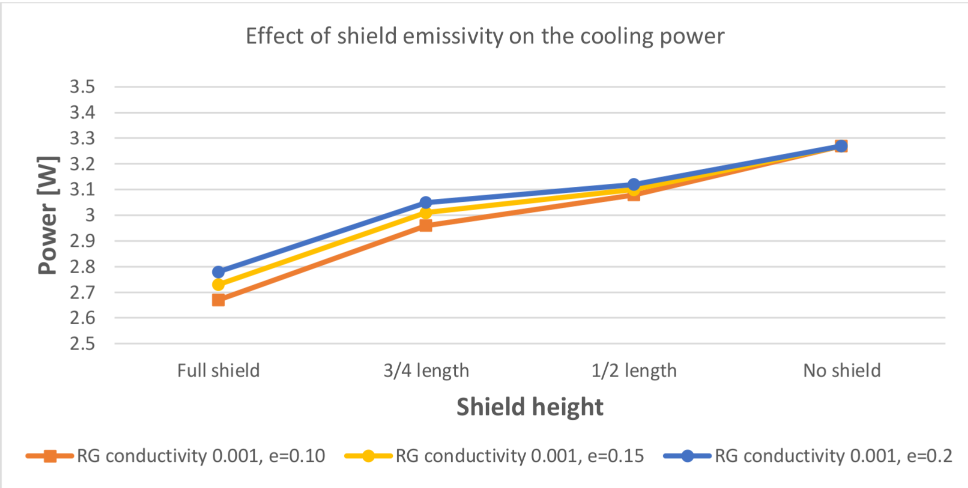

Figure 8. Effect of shield emissivity (e) on the cooling power at different shield heights. Residual Gas (RG) conductivity is always 0.001 W/m/K.

Figure 9 shows the surface average temperature of the shield and detector with varying shield emissivity and height.

It can be seen that using a shield (of any length and surface emissivity) decreases the detector compartment surface temperature. Same is true for the shield temperature, however, the temperature decreases with shield height more slowly using higher emissivity (i.e. less reflective surface). In all varied emissivity sets, the average detector temperature (87.7 K) is ~2 degrees higher in the system where no shield was used compared to the system where the shield was used (85.9 K). Similarly,

2020 JINST 15 P01026

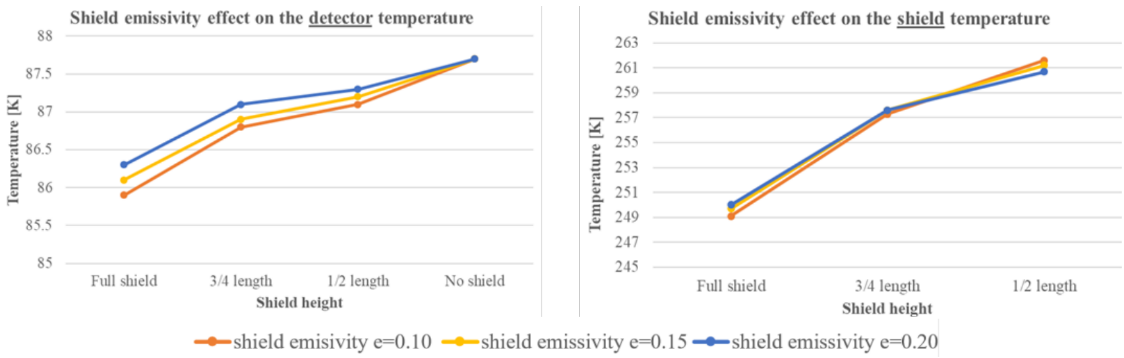

Figure 9. Surface average temperature of the detector container and the shield.

50% shield height showed average shield temperature (261.6 K) which is 12.1 K higher than in the full-length shield system (249.1 K).

The message relayed from these results is that a shield has a significant positive effect on the cooling requirements and therefore on the operating time.

4.4 Effect of the vacuum level

In order to evaluate the effect of vacuum level on the shield temperature field, we simulated two cases — one with a high vacuum (~1E-5 mbar) and another one with a low vacuum (~1E-3 mbar) in the cryostat. The resulting temperature fields are shown in figure 10.

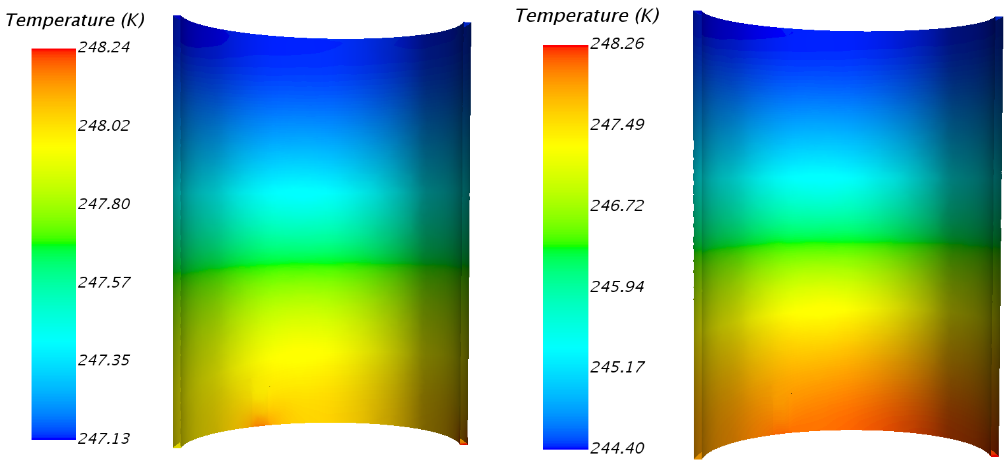

a) — high vacuum

b) — low vacuum

Figure 10. Temperature distribution on the shield at a) high (~1E-5 mbar) and b) low (~1E-3 mbar) vacuum conditions.

The temperature at the bottom of the shield where it is connected to its support structures remains largely unchanged (about 248.3 K) in different vacuum levels. However, the range of temperature on the shield is different in those cases:

- in the case of high vacuum, the range is ~1 K.
- in case of low vacuum, the range is ~4 K.

It was observed that the required cooling power increases up to 2 times in the low vacuum case compared to high vacuum case, corresponding to the earlier finding that the effect of radiation shield on the cooling power is more pronounced at the highest vacuum condition in the cryostat (<1E-4 mbar).

4.5 Validation against measurements in the cool-down test

Experimental investigations of the cryostat-prototype performance were carried out using Thales LSF 9589 cryocooler providing 2.7 W of cooling power at 80 K.

In order to validate the results of the numerical model, a time-dependent cool-down test was performed experimentally and simulated. Testing the full cryostat model allows to study the dynamics of the heat flows and temperature changes in all the parts of the detector. Moreover, transient simulation provides confidence in the reliability of the previously built steady-state model i.e. its performance concerning thermal inertia. In particular, the cooling of the spectrometer from room temperature to the operating/cryostatic temperature (~70 K) is simulated. Comparison of the simulated and experimentally measured temperature in certain locations in the spectrometer is shown in figure 11.

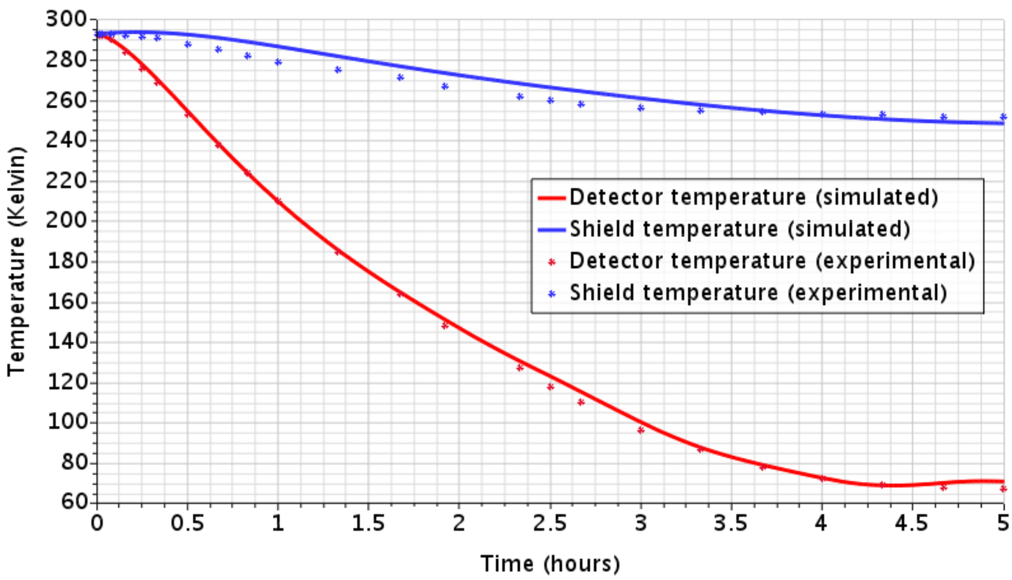

Figure 11. Simulated and experimentally measured cool-down of the HandSpec spectrometer.

Figure 11 shows that simulation is able to predict detector temperature evolution during the cool-down process reasonably well. A small deviation in the shield temperature can be attributed to the uncertainty in the temperature measurement/monitor location.

5 Conclusions

This work presents the results of heat transfer analysis in a cryostat using a thermal shield in its vacuum chamber to improve the efficiency of the spectrometer. A detailed numerical model is built in a commercial CFD software Star-CCM+ according to the CAD drawings and design specifications provided by the manufacturer. Model verification, calibration and validation are carried out.

Three-dimensional simulations were used to evaluate the relative contribution of different heat transfer mechanisms to the overall heat leak from the environment to the detector and cooler. Several sensitivity studies concerning the required cooling power, detector temperature and shield temperature distribution were carried out. It was found that thermal conduction through structural materials has the lowest relative contribution (0.1–0.3 W), lowest uncertainty and minimized by design as much as possible. Moreover, high vacuum is a pre-requisite for the efficient performance of the spectrometer i.e. corresponding to cooler power in the order of 2–3 W. Having sufficiently low pressure in the vacuum chamber, heat leak can be further reduced by using a reflective thermal shield.

The steady state and transient analysis results compare reasonably well with experimentally observed values confirming that the 3D model reflects physical reality sufficiently to be used as a heat transfer analysis tool in spectrometer development.

Acknowledgments

This work has been carried out within the project "Hand-held spectrometer design" (HADEDE) supported by the cross-border cooperation program Interreg V-A — Estonia–Latvia, co-funded by the European Regional Development Fund. The paper reflects the views of the authors; the managing authority of the program is not liable for how this information may be used.

References

[1] D.L. Upp, R.M. Keyser and T.R. Twomey, *New cooling methods for HPGE detectors and associated electronics*, *J. Radioanal. Nucl. Chem.* **264** (2005) 121.

[2] R.M. Keyser and R.C. Hagenauer, *Performance of a portable, electromechanically-cooled HPGe detector for site characterization*, *J. Radioanal. Nucl. Chem.* **277** (2008) 149.

[3] V. Parma, *Cryostat design*, arXiv:1501.07154.

[4] M. Katagiri, T. Senzaki, A. Birumachi and T. Kozawa, *In-situ gamma-ray spectrum monitoring system using a compact electrically-cooled Ge detector*, in *ICONE-7: 7^{th} international conference on nuclear engineering*, Tokyo Japan (1999).

[5] M. Katagiri, A. Birumachi, K. Sakasai and K. Takahashi, *Portable Gamma-ray Monitor Composed of a Compact Electrically Cooled Ge Detector and a Mini-MCA System*, *IEEE Nucl. Sci. Symp. Med. Imag. Conf.* **2002** (2002) 1.

[6] E.L. Hull et al., *Mechanically cooled large-volume germanium detector systems for nuclear explosion monitoring*, in *Proceedings of the 28th Seismic Research Review: Ground-Based Nuclear Explosion Monitoring Technologies*, Los Alamos U.S.A. (2006).

[7] K.M. Yocum, G.N. Martin, J.F. Colaresi and H.S. Miley, *Improvement in Ge detector cooling*, Canberra Industries Meriden CT, Canberra Australia (2008).

2020 JINST 15 P01026

[8] Y.-S. Choi, D.-L. Kim and D.-W. Shin, *Estimation of Cooldown Time in Cryocooled Superconducting Magnet System*, *Prog. Supercond. Cryog.* **12** (2010) 25.

[9] I. Kojouharov, J. Gerl, A. Sanchez-Lorente, M. Steinen, J. Pochodzalla and J. Kojouharova, *Optimization of Electrically Cooled Complex HPGe Detector*, in *Sixth UKSim/AMSS European Symposium on Computer Modeling and Simulation (EMS 2012)*, Valetta Malta (2012), pg. 461.

[10] B. Baudouy, *Heat Transfer and Cooling Techniques at Low Temperature*, in *Proceedings, CAS — CERN Accelerator School: Course on Superconductivity for Accelerators (CAS 2013)*, Erice Italy (2013), pg. 329.

[11] SIEMENS, *Simcenter STAR-CCM+® Documentation*, Version 13.02 (2018).

2020 JINST 15 P01026